Synthesis and Crystal Structure of the Pentahydrated Uranyl Orthovanadate $(UO_2)_3(VO_4)_2 \cdot 5H_2O$, Precursor for the New $(UO_2)_3(VO_4)_2$ Uranyl-Vanadate

M. Saadi, C. Dion, and F. Abraham[1]

Laboratoire de Cristallochimie et Physicochimie du Solide, UPRESA 8012, ENSCL, Université des Sciences et Technologies de Lille, B.P. 108, 59652 Villeneuve d'Ascq Cedex, France

The pentahydrated uranyl orthovanadate $(UO_2)_3(VO_4)_2 \cdot 5H_2O$ was synthesized in shaken aqueous solution at 60°C, by reaction of UO_3 or a uranyl salt (acetate or nitrate) and V_2O_5. Single crystals were obtained by hydrothermal reaction at 180°C. It crystallizes in an orthorhombic system, space group *Cmcm*, with $a = 17.978(2)$ Å, $b = 13.561(2)$ Å, $c = 7.163(1)$ Å, $V = 1746.3$ Å^3, $Z = 4$, $\rho_{cal} = 4.3$ g·cm^{-3}. The structure has been refined to $R = 0.048$ and Rw $= 0.047$ using 1020 independent reflections with $I > 3\sigma(I)$ collected on a Philips PW 1100 automated diffractometer using Mo$K\alpha$ radiation. Uranyl ions have two distinct functions. $U(1)O_2^{2+}$ uranyl ions are surrounded in an equatorial plane by five oxygen atoms of four different VO_4 tetrahedra which form pentagonal UO_7 bipyramids. The linkage of UO_7 bipyramids and VO_4 tetrahedra leads to $(UVO_6)_\infty$ layers parallel to the (100) plane. The connection between these sheets is achieved by the other $U(2)O_2^{2+}$ uranyl ions and water molecules. Thus, the compound may be considered a uranyl vanadate of uranyl and can be formulated $(UO_2)_{0.5}[(UO_2)(VO_4)] \cdot 2.5H_2O$. Dehydration is reversible and leads to a new anhydrous compound $(UO_2)_3(VO_4)_2$ after intermediate steps corresponding to different hydrates. Unfortunately, the anhydrous product cannot be synthesized directly from UO_3 and V_2O_5 by solid-state reaction. © 2000 Academic Press

INTRODUCTION

Uranyl vanadates and uranyl phosphates show many similarities. Both belong to the large class of compounds with the general formula $M_{1/n}^{n+}(UO_2)XO_4 \cdot xH_2O$, where M can be most mono, di, or trivalent cations (1). They are structurally characterized by a layered structure; M^{n+} ions and H_2O molecules occupy the interlayer space between $[(UO_2)(XO_4)]_\infty$ sheets. However, the building of the layers is different for the two chemical families: in phosphate

compounds, the UO_2^{2+} ions are linked by PO_4^{3-} tetrahedra (2), whereas in V compounds, they are bridged by centrosymmetric $V_2O_8^{6-}$ units formed from two inverse VO_5 square pyramids sharing an edge (3–6). Therefore the V-compounds have to be formulated $M_{2/n}^{n+}(UO_2)_2V_2O_8 \cdot xH_2O$.

Hydrogen uranyl phosphate tetrahydrate $HUO_2PO_4 \cdot 4H_2O$ (HUP) displays a good selective proton conductivity at room temperature in relation to its layered structure and is interesting for its potential applications in electrochemical systems (7–10).

By comparison, $H_2(UO_2)_2V_2O_8 \cdot xH_2O$ (HUV) should be a good protonic electrical conductor. This vanadate has been reported only by Barton (11). It is irreversibly decomposed at 470°C into uranyl divanadate $(UO_2)_2V_2O_7$ (12). Although it is not well characterized, its numerous hydrated and anhydrous salts $M_{2/n}^{n+}(UO_2)_2V_2O_8 \cdot xH_2O$ (with $M =$ Na, K, Rb, Cs, Ag, Tl, NH_4 for monovalent cations and $M =$ Ca, Ba, Sr, Pb, Mn, Co, Ni, for divalent cations) are well identified (13, 4). For instance, the Carnotite $K_2(UO_2)_2V_2O_8$ is an uranium ore.

In the course of the hydrated HUV preparation, we obtained a new uranyl vanadate $(UO_2)_3(VO_4)_2 \cdot 5H_2O$. Its dehydration led to the up to today unknown uranyl orthovanadate.

Three compounds belong to the UO_3–V_2O_5 system, $UVO_{5.5}$ (or $U_2V_2O_{11}$), UV_2O_8, and $U_2V_6O_{21}$. The two firsts are obtained by direct reaction between oxides UO_3 and V_2O_5 at 650°C under oxygen atmosphere. The last $U_2V_6O_{21}$ (or $UV_3O_{10.5}$) results from slow oxidation of UV_3O_{10} under oxygen flow at 550°C (14).

Moreover, three partially reduced mixed oxides have been found: UVO_5 and UV_3O_{10} are prepared by reaction between UO_3 or U_3O_8 and V_2O_5 at 650°C under vacuum or by reduction of $UVO_{5.5}$ and UV_2O_8 under vacuum (14); UV_2O_6 is obtained from a UO_2 and V_2O_5 mixture heated between 900 and 1200°C under argon (15). UVO_5 and UV_3O_{10} have also been synthesized from mixtures of V_2O_3,

[1] To whom correspondence should be addressed. E-mail: abraham@ensc-lille.fr.

V_2O_5, and α-U_3O_8 in stoichiometric proportions heated in sealed, evacuated silica tubes at 700 and 550°C, respectively (16, 17).

The structure of UV_2O_8 previously described as built from UO_6 pentagonal pyramids and V_2O_8 units formed by two VO_5 trigonal pyramids sharing an edge (18, 19) has been recently revisited by powder neutron diffraction (20); actually, the structure consists of UO_7 pentagonal bipyramids and VO_4 tetrahedra sharing corners to give infinite metavanadate chains.

The crystal structure of $U_2V_2O_{11}$ has been solved recently *ab inito* from powder X-ray diffraction data (21) and simultaneously by using single-crystal X-ray and powder neutron diffraction (20). The network is built from $V_2O_7^{4-}$ divanadate ions (resulting from the association of two VO_4 tetrahedra sharing a corner) and UO_2^{2+} uranyl cations. The coordination polyhedra of uranium atoms is a UO_7 pentagonal bipyramid. $U_2V_2O_{11}$ can be considered a uranyl pyrovanadate $(UO_2)_2V_2O_7$.

The crystal structures of UVO_5, previously determined from single-crystal X-ray data (22, 23), and UV_3O_{10} have been recently refined using Rietveld analysis of combined powder neutron and powder X-ray data (16, 17).

In the present paper, the synthesis and crystal stucture determination of the new uranyl vanadate $(UO_2)_3(VO_4)_2 \cdot 5H_2O$ and its thermal stability are reported.

EXPERIMENTAL

Syntheses

With the aim of synthesizing $HUV \cdot xH_2O$, several attempts were made:

(i) An equimolar mixture of $UO_3 \cdot 1H_2O$ or uranyl salt (acetate or nitrate) and V_2O_5 was shaken in aqueous solution at 60°C for 15 days. After filtration, washing with distilled water, and drying, a yellow powder was obtained.

(ii) For the hydrothermal method at 180°C, an equimolar mixture of $UO_3 \cdot 1H_2O$ or uranyl acetate and V_2O_5 (4×10^{-4} mol) was introduced in a glass tube two-thirds filled with water and sealed. Heating at 180°C for 8 days gave rise to the same yellow powder characterized by X-ray powder diffraction.

(iii) Under the same conditions used previously (ii), from an equimolecular mixture of uranyl nitrate and V_2O_5, yellow single crystals and a poorly crystallized unidentified orange-colored powder were obtained. The X-ray powder diffraction of the crushed crystals corresponds to the major part of the pattern obtained from the yellow powders. Actually, the yellow powder obtained in (i) and (ii) contains an unknown second phase.

The crystal structure determination of the yellow single crystals revealed the formula $(UO_2)_3(VO_4)_2 \cdot 5H_2O$. Finally, pure yellow powder of this compound was synthesized by methods (i) and (ii) from stoichiometric mixtures U/V = 3/2.

With method (i) the powder was poorly crystallized, whereas method (ii) led to well-crystallized powder used for unit cell parameters refinement from X-ray powder diffraction data.

Structure Determination

A yellow single crystal was selected for the structure determination. Preliminary oscillation and Weissenberg photographs indicated an *mmm* Laue symmetry. Systematic absences of reflections *hkl*, $h + k = 2n + 1$, and *h0l*, $l = 2n + 1$ were consistent with $C2cm$, $Cmc2_1$, and $Cmcm$ space groups. Finally, the structure was solved in the centrosymmetric Cmcm space group.

The intensity data were collected on a Philips PW 1100 automated diffractometer. Conditions for data collection are given in Table 1. The intensity of each reflection was corrected for background and for Lorentz and polarization

TABLE 1
Crystal Data, Intensity Collection and Structure Refinement Parameters for the $(UO_2)_3(VO_4)_2 \cdot 5H_2O$ Single Crystal

Crystal data:	
Crystal symmetry	orthorhombic
Space group	*Cmcm*
Unit-cell parameters	$a = 17.978(2)$ Å
	$b = 13.561(2)$ Å
	$c = 7.163(1)$ Å
Volume	1746.3 Å^3
Z	4
Calculated density	4.3 g/cm^3
Data collection:	
Equipment	Philips PW 1100
$\lambda Mo_{K\alpha}$ radiation	0.7107 Å
Scan mode	$\omega - 2\theta$
Scan width (°)	1.2
θ range (°)	2–30
Recording reciprocal space	$-25 \leq h \leq 25, -19 \leq k \leq 19,$
	$0 \leq 1 \leq 10$
Standard reflections	$00\bar{2}, 202, \bar{2}41$
Number of measured reflections	5455
Number of reflections $I > 3\sigma(I)$	3444
Number of independent reflections	1020
μ (cm^{-1}) (for $\lambda K\alpha = 0.7107$ Å)	277
Limiting faces and distances (cm)	$100, \bar{1}00$ 0.0006
From an arbitrary origin	$010, 0\bar{1}0$ 0.0032
	$001, 00\bar{1}$ 0.0106
Transmission factor range	0.04–0.56
R merging factor	0.058
Refinement parameters	
Number of refined parameters	49
Goof = S (goodness of fit)	2.4
$R = \sum[|F_o| - |F_c|]/\sum|F_o|$	0.048
$Rw = [\sum w(|F_o| - |F_c|)^2/\sum F_o^2]^{1/2}$	
with $w = 1/\sigma(F_o)$	0.047

effects. Absorption corrections were performed using the analytical method of De Meuleaner and Tompa (24).

The structure was solved by the heavy atom method. The calculation of the Patterson function allowed us to localize the first uranium atoms U(1) in the 8g site (0.22; 0.06; 1/4). After refinement of these coordinates, a second site was revealed in a Fourier difference synthesis at 8f (0; 0.75; 0.12). The two equivalent positions related by the m mirror perpendicular to [001] are too close (1.8 Å) and cannot be simultaneously occupied, and the 8f site was considered, after several hypotheses, as half occupied by a uranium atom U(2). Vanadium atoms were then localized in 8g (0.80; 0.82; 1/4). The reliability factors were under the conditions $R = 0.14$ and $Rw = 0.20$.

Two subsequent Fourier difference syntheses showed four 8g sites and one 16h site occupied by oxygen atoms around U(1) and V(1), and two 8f sites for oxygen atoms with half occupation in the surroundings of U(2).

A new Fourier difference synthesis allowed us to localize two 16h sites half occupied by oxygen atoms of water molecules. The oxygen atom of the last water molecule was not deduced from the Fourier synthesis; its coordinates were calculated to complete the coordination polyhedron around U(2). The formula was finally $U_3V_2O_{14} \cdot 5H_2O$. The absorption corrections were improved at this stage with the actual absorption coefficient calculated for this formula. Least-squares refinement of the positional parameters and anisotropic (U,V atoms) or isotropic (O atoms) thermal parameters leads to discrepancy factors, $R = 0.048$ and $Rw = 0.047$. The atomic coordinates and isotropic displacement parameters are given in Table 2. The displacement temperature parameters for U and V atoms are reported in Table 3.

Scattering factors were taken from the International Tables for X-Ray Crystallography (25). The anomalous dispersion corrections were made according to Cromer and Liberman data (26). The full matrix least-squares refinements were performed with a local modification of SFLS-5 (27).

The unit cell parameters reported in Table 1 were refined from X-Ray powder patterns obtained with a Siemens D 5000 diffractometer (CuKα radiation) equipped with a monochromator and corrected for $K\alpha_2$ contribution. The figure of merit, as defined by Smith and Snyder (28), was $F_{20} = 132$ (0.0063, 24). The powder X-ray diffraction pattern data are reported in Table 4.

Thermal Analysis

Thermogravimetric analysis (TG) was conducted in air with a Dupont 951 instrument at a heating rate of $0.3°C \cdot min^{-1}$; differential thermal analysis was performed with a Dupont 910 differential scanning calorimeter, at a heating rate of $10°C \cdot min^{-1}$. The X-ray powder diffraction

pattern versus temperature was obtained with a Guinier–Lenné focusing camera using CuKα radiation

RESULTS AND DISCUSSION

Description and Discussion of the Crystal Structure

Selected bond lengths and bond angles are listed in Table 5.

In this compound the U(1) atom is surrounded by a pentagonal bipyramidal arrangement of oxygen atoms. The U(1)–O(1) and U(1)–O(2) distances of 1.75–1.76 Å and the O(1)–U(1)–O(2) angle unambiguously indicate the existence of symmetrical linear uranyl ions $U(1)O_2^{2+}$. The coordination of the uranium atom is completed in the plane perpendicular to the O=U(1)=O group by five equatorial oxygen atoms, four O(4) and one O(3), more distant, with average $d_{U-O(eq)} = 2.38$ Å, characteristic for U^{VI} in this environment. UO_7 pentagonal bipyramids are associated together

TABLE 2
Atomic Positions, Thermal Isotropic Factors (O), and Equivalent Isotropic Temperature Factors (U, V) for $(UO_2)_3(VO_4)_2 \cdot 5H_2O$

Atom	Site	Ocup. rate	x	y	z	B or B_{eq} (Å^2)
U(1)	8g	1	0.22400(4)	0.06276(5)	1/4	1.30(1)
U(2)	8f	1/2	0	0.7552(1)	0.3815(2)	2.91(4)
V	8g	1	0.7913(1)	0.8253(2)	1/4	1.42(6)
O(1)	8g	1	0.1268(7)	0.065(1)	1/4	2.8(2)
O(2)	8g	1	0.3218(9)	0.057(2)	1/4	4.1(3)
O(3)	8g	1	0.2273(6)	0.2326(9)	1/4	1.9(2)
O(4)	16h	1	0.2218(6)	0.0933(8)	0.571(2)	3.6(2)
O(5)	8g	1	0.124(1)	0.782(2)	1/4	6.1(5)
O(6)	8f	1/2	0	0.864(4)	0.463(7)	7(1)
O(7)	8f	1/2	0	0.658(4)	0.313(5)	6(1)
H$_2$O(1)	16h	1/2	−0.076(3)	0.700(5)	0.637(7)	12(2)
H$_2$O(2)	16h	1/2	−0.082(2)	0.610(3)	−0.055(6)	8.2(9)
H$_2$O(3)	8f	1/2	0	0.823	0.067	

Note. Equivalent isotropic temperature factors are computed according to the relation $B_{eq} = 4/3\sum_{ij}\beta_{ij}a_ia_j$.

TABLE 3
Anisotropic Thermal Factors ($\times 10^4$) (U, V) for $(UO_2)_3(VO_4)_2 \cdot 5H_2O$

Atom	U_{11}	U_{22}	U_{33}	U_{12}	U_{13}	U_{23}
U(1)	264(3)	78(2)	151(2)	−10(3)	0	0
U(2)	213(6)	428(10)	467(9)	0	0	−48(8)
V	251(12)	92(13)	196(14)	−13(9)	0	0

Note. The temperature factor is defined by $\exp[-2\pi^2\alpha(U_{11}h^2a^{*2} + \cdots + 2U_{23}klb^*c^*)]$.

TABLE 4
Observed and Calculated X-Ray Powder Pattern for
$(UO_2)_3(VO_4)_2 \cdot 5H_2O$

h k l	$2\theta_{obs}$	$2\theta_{cal}$	I_{obs}	h k l	$2\theta_{obs}$	$2\theta_{cal}$	I_{obs}
1 1 0	8.179	8.183	1	7 1 0	35.571	35.570	11
2 0 0	9.851	9.855	23	5 1 2	36.007	36.002	2
0 2 0	13.08	13.069	2	7 1 1	37.795	37.790	6
1 1 1	14.833	14.840	5	3 5 1	38.539	38.532	8
3 1 0	16.162	16.170	22	1 1 3	38.605	38.606	1
2 2 0	16.392	16.385	37	6 0 2	39.205	39.191	1
0 2 1	18.027	18.022	4	0 6 0	39.880	39.875	2
4 0 0	19.763	19.759	100	0 2 3	40.024	40.025	1
3 1 1	20.410	20.408	4	8 0 0		40.114	
2 2 1	20.556	20.572	8	6 4 0	40.134	40.153	5
1 3 1	23.804	23.780	4	3 1 3	41.229	41.230	1
0 0 2	24.869	24.864	4	2 2 3	41.316	41.317	1
5 1 0	25.619	25.633	26	0 6 1	41.890	41.900	1
1 1 2	26.210	26.210	<1	6 4 1	42.180	42.168	1
0 4 0	26.300	26.288	<1	8 2 0		42.359	
2 0 2	26.798	26.797	9	7 3 1	42.378	42.386	2
4 2 1	26.862	26.857	3	2 6 1	43.144	43.146	2
2 4 0	28.130	28.130	2	5 5 1	43.660	43.657	1
0 2 2	28.180	28.179	1	7 1 2	43.873	43.876	4
5 1 1	28.540	28.546	3	3 5 2	44.544	44.534	1
0 4 1	29.136	29.140	9	4 6 0	44.858	44.873	2
3 1 2		29.798		4 2 3	45.007	45.009	1
6 0 0	29.799	29.816	3	3 3 3	45.529	45.539	2
2 2 2	29.918	29.913	2	9 1 0	45.889	45.904	12
2 4 1	30.824	30.825	11	5 1 3	46.106	46.108	1
4 0 2	31.952	31.949	2	0 4 3	46.503	46.505	2
6 2 0	32.669	32.670	8	4 6 1	46.720	46.722	1
4 4 0	33.086	33.092	1	2 4 3	47.644	47.654	3
4 2 2	34.657	34.644	1	8 4 0	48.586	48.588	1
6 2 1	35.062	35.050	1	2 6 2	48.683	48.685	<1
4 4 1	35.448	35.447	4	7 5 1	50.561	50.555	4

Note. $\lambda = 1.54056\,\text{Å}$, refined zero-point correction 0.011(2) for θ; $a = 17.978(2)\,\text{Å}$; $b = 13.561(2)\,\text{Å}$; $c = 7.163(1)\,\text{Å}$; $F_{20} = 132$ (0.0063, 24).

through the oxygen atoms of the basal plane of the UO_7 bipyramids. A UO_7 bipyramid shares two opposite O(4)–O(4) edges with two other UO_7 bipyramids to form zig-zag infinite chains $(UO_5)_\infty$ running along the c axis (Fig. 1). Vanadium is tetrahedrally coordinated. Two parallel chains at $x = 0.224$ and $x = 0.276$ are connected by VO_4 tetrahedra. A VO_4 tetrahedron shares the O(4)–O(4) edge with a UO_7 bipyramid of one chain and a O(3) corner with a UO_7 polyhedron of the other chain. The O(5) atom strongly bonded to the vanadium atom is not involved in the U(1) coordination. The chains so connected by VO_4 tetrahedra constitute slightly corrugated layers with formula $[U(1)O_2(VO_4)]_\infty$ parallel to the (100) plane (Fig. 1). The separation between adjacent layers is $a/2$. In fact, the absence of discrete vanadate tetrahedra leads us to consider charged extended covalent layers $[(UVO_6)^-]_\infty$.

The oxygen arrangement around the vanadium atom is strongly distorted with a V–O(5) bond significantly shorter

than the other vanadium–oxygen distances, and the O(5) atom is not involved in the formation of the layers. The O(4)–O(4) edge shared between VO_4 and UO_7 polyhedra is shorter (2.54 Å) than the other O–O edges which are not shared, according to the theory of Pauling (29) and Baur (30), so the O(4)–V–O(4) angle is particularly lower than 109.7°.

Similar chains of edge-shared UO_7 polyhedra have been described in other uranium oxides, but the connection of parallel chains to form layers is different. The stacking of the layers is also different. For example, in α-U_3O_8 (31), the chains are directly attached by corner sharing (Fig. 2a), pentagonal and trigonal sites are produced between the chains, pentagonal sites are occupied by U atoms, and trigonal sites are empty. In UVO_5 (16), a compound containing U^V, $(UO_5)_\infty$ chains share edges with square bases of VO_5 square-pyramids (Fig. 2b). The resulting layers are stacked in registry by perpendicular chains containing –U–O–U–O– and –V–O–V–O–. $USbO_5$ (32) resembles

TABLE 5
Bond Distances (Å) and Selected Bond Angles (°) for
$(UO_2)_3(VO_4)_2 \cdot 5H_2O$

U(1) environment			
U(1)–O(1)	1.75(1)	O(1)–U(1)–O(3)	90.5(6)
U(1)–O(2)	1.76(2)	O(1)–U(1)–O(4) (2×)	88.9(4)
U(1)–O(3)	2.30(1)	O(1)–U(1)–O(4)$_{001}^{ii}$ (2×)	89.9(5)
U(1)–O(4) (2×)	2.34(1)	O(2)–U(1)–O(3)	91(1)
U(1)–O(4)$_{001}^{ii}$ (2×)	2.47(1)	O(2)–U(1)–O(4) (2×)	91.4(5)
O(1)–U(1)–O(2)	178(1)	O(2)–U(1)–O(4)$_{001}^{ii}$ (2×)	88.7(9)
U(2) environment			
U(2)–O(6)	1.59(5)	$H_2O(1)$–U(2)–$H_2O(1)$	69(2)
U(2)–O(7)	1.41(5)	O(6)–U(2)–O(7)	179(3)
U(2)–O(5) (2×)	2.45(2)	O(6)–U(2)–O(5) (2×)	90(1)
U(2)–$H_2O(1)$ (2×)	2.40(5)	O(6)–U(2)–$H_2O(1)$ (2×)	91(3)
O(5)–U(2)–O(5)	131.3(7)	O(7)–U(2)–O(5) (2×)	90(1)
O(5)–U(2)–$H_2O(1)$	80(1)	O(7)–U(2)–$H_2O(1)$ (2×)	89(2)
V Environment			
V–O(3)^{ix}	1.70(1)	O(3)^{ix}–V–O(4)$_{111}^{v}$ (2×)	112.6(7)
V–O(4)$_{111}^{v}$ (2×)	1.71(1)	O(3)^{ix}–V–O(5)$_{100}^{vi}$	111(1)
V–O(5)$_{100}^{vi}$	1.63(2)	O(4)$_{111}^{v}$–V–O(4)$_{11\bar{1}}^{vii}$	97.3(8)
		O(4)$_{111}^{v}$–V–O(5)$_{100}^{vi}$ (2×)	111.2(9)
H_2O molecules environment			
$H_2O(1)$–O(3)$_{001}^{v}$	2.98(6)	$H_2O(1)$–$H_2O(1)^{vi}$	2.73(10)
$H_2O(1)$–O(6)	2.89(8)	$H_2O(3)$–O(1)$_{010}^{i}$ (2×)	2.88(7)
$H_2O(1)$–O(7)	2.75(6)	$H_2O(3)$–O(6)	2.61(12)
$H_2O(1)$–O(5)^{vi}	3.11(5)	$H_2O(3)$–O(5) (2×)	3.27(8)
$H_2O(1)$–$H_2O(2)_{001}^{i}$	2.52(7)	$H_2O(3)$–O(6)$_{02\bar{1}}^{iv}$	3.07(13)
$H_2O(2)$–O(2)$_{\bar{1}00}^{ix}$	2.88(4)		
$H_2O(2)$–O(2)$_{\bar{1}00}^{x}$	3.17(4)		
$H_2O(2)$–$H_2O(1)_{00\bar{1}}$	2.52(7)		
$H_2O(2)$–O(7)	3.09(5)		

Note. $O(n)_{pqr}^m$ represents atom $O(n)$ for the symmetry m and the translation $pa + qb + rc$. Symmetry codes: (i) x, y, z; (ii) $x, \bar{y}, \bar{z}$; (iii) $x, y, 1/2 - z$; (iv) $x, \bar{y}, 1/2 + z$; (v) $\bar{x}, \bar{y}, \bar{z}$; (vi) $\bar{x}, \bar{y}, z$; (vii) $\bar{x}, \bar{y}, 1/2 + z$; (viii) $\bar{x}, y, 1/2 - z$.
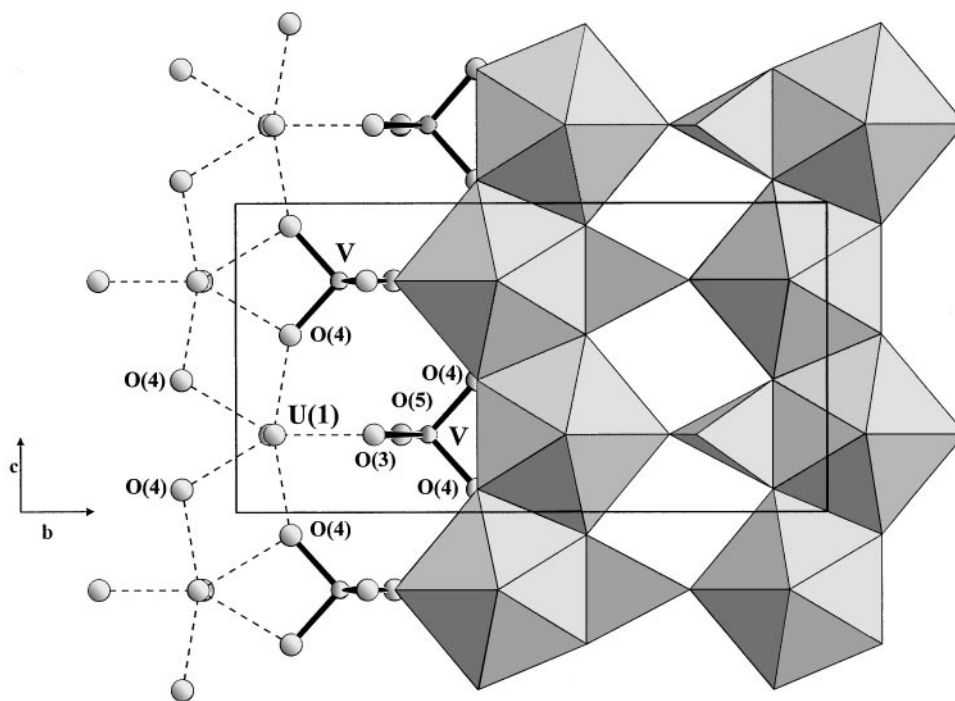
FIG. 1. The crystal structure of $U_3V_2O_{14} \cdot 5H_2O$ in the (100) plane showing how the $(UVO_6)_\infty$ layers form from edge-shared uranium pentagonal bipyramids and vanadium tetrahedra.

UVO_5 in its intralayer arrangement but differs in the stacking of the layers; displacement of successive layers leads to heterometallic –U–O–Sb–O–U–O–Sb– chains. In these compounds, no uranyl grouping is present, the U–O bond lengths along the chains perpendicular to the layers are greater than 2.0 Å. In the orthorhombic modification of UMo_2O_8 (33) and the recently published isotypic $U(Ta,W)_2O_8$ series (34), the $(UO_5)_\infty$ chains are intergrown with ReO_3-type slabs of tilted octahedra, two MoO_6 octahedra wide (Fig. 2c). As in UVO_5, the layers of heavy atoms are connected by monometallic –M–O–M– infinite chains. In $U_2V_2O_{11}$ (20, 21), $(UO_5)_\infty$ chains are connected by divanadate V_2O_7 entities to form layers (Fig. 2d). The obtained corrugated layers are joined by linear V–O–V units to form a three-dimensional structure; in this case the oxygen atoms of the UO_2 group are uninvolved in the interlayer bonding, and the uranyl group remains free with two short U–O bond lengths (1.72 and 1.77 Å). The distances calculated for the chains in the different oxides are compared in Table 6.

Finally, the $(UVO_6)_\infty$ layers observed in our compound are very similar to the layers formed between $(UO_5)_\infty$ chains and PO_4 tetrahedra in $U_2P_2O_{10}$ (35). In $U_2P_2O_{10}$ the $(UO_5)_\infty$ chains are more distorted, in fact they are formed from two types of UO_7 bipyramids, containing uranium atoms at oxydation states +4 and +6 for $U(1)O_7$ and

$U(2)O_7$, respectively, following one another in the $[U(1)_2–U(2)_2]$ sequence. In $U_2P_2O_{10}$, the layers are parallel to the $(11\bar{1})$ plane and the dimensions of the pseudo-rectangular lattice (Fig. 3) calculated from the triclinic cell of $U_2P_2O_{10}$ ($\mathbf{a}'$, $\mathbf{b}'$, $\mathbf{c}'$) compared well with those of the present compound ($|\mathbf{b}' - \mathbf{a}'| = 14.07$ Å compared with $2c = 14.33$ Å; $|\mathbf{a}' + \mathbf{b}' + 2\mathbf{c}'| = 13.32$ Å compared with $b = 13.56$ Å; the angle for the pseudo-rectangular lattice is 90.58°). Although the O–O common edges between UO_7 and PO_4 are shorter than the one in $(UVO_6)_\infty$ layers, the O–P–O angles are greater than the corresponding O–V–O angle since the P–O bond lengths are significantly shorter than the V–O bonds. The $U(2)O_2$ uranyl group is uninvolved in the interlayer bonding and remains free with U–O distances of 1.76 Å. Of course for U^{IV} there is no uranyl bond; the bond lengths are longer (2.17 Å). Two successive layers are linked together by limited P–O–U^{IV}–O–P entities running perpendicular to them. The common oxygen atoms are not involved in the layer formation.

In contrast, in the title compound, there is no direct interaction between consecutive layers. The layers are linked together by other uranyl ions $[U(2)O(6)O(7)]^{2+}$ located in planes parallel to (100), respectively, at $x = 0$ and $x = 0.50$ (Fig. 4). The O(6)–U(2)–O(7) angle is nearly 180°, but the U=O bond lengths are particularly short. These abnormally short lengths can result from the disorder affect-
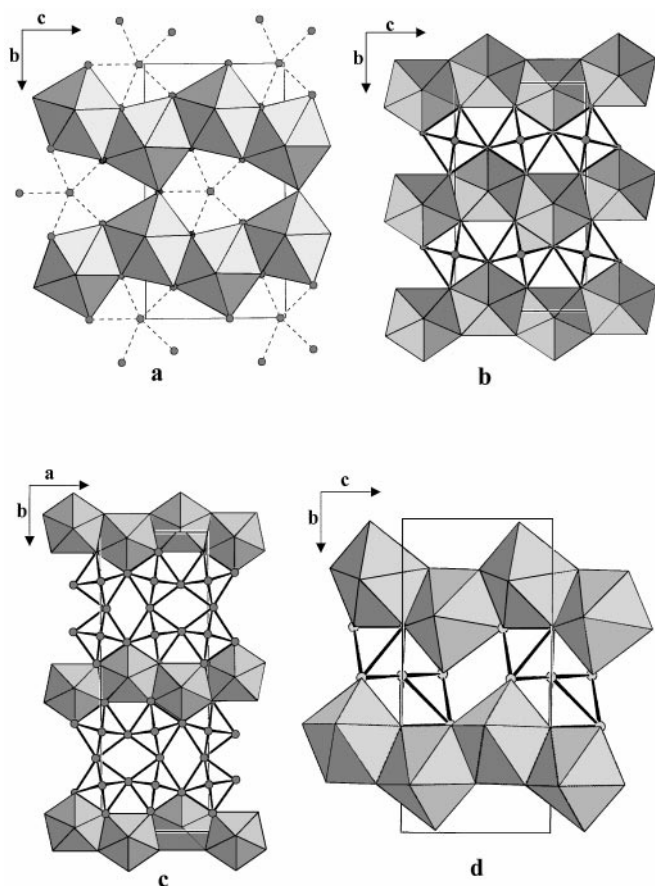
FIG. 2. The connection between zig-zag chains of UO_7 pentagonal bipyramids sharing opposite edges (a) by corner sharing in U_3O_8, (b) by VO_5 square pyramids or octahedra in UVO_5 or $USbO_5$, respectively, (c) by ReO_3-type slabs two octahedra wide in UMo_2O_8, (d) by divanadate groups in $U_2V_2O_{11}$.
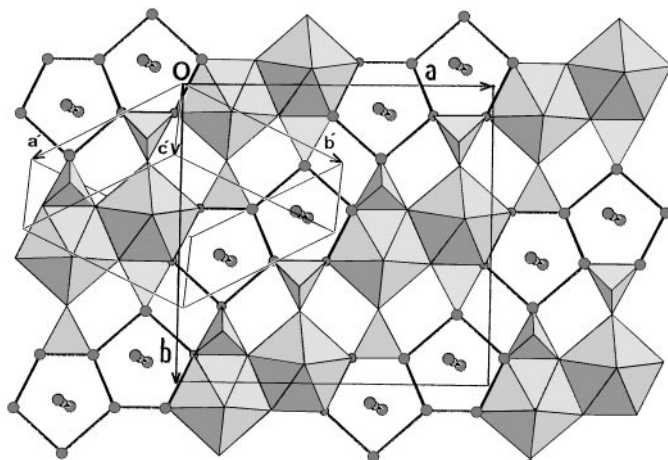
TABLE 6
Characteristic Distances in $(UO_5)_\infty$ Chains in Different Compounds

	(U–U)	(O–O)	(U–O_{ax})	$\langle U-O_{eq}\rangle$	Ref.
$(UO_2)_3(VO_4)_2 \cdot 5H_2O$	3.90(1)	2.70(2)	1.77(1); 1.76(1)	2.38	
U_3O_8	3.79(1)	2.57(1)	2.07(1); 2.07(1)	2.28	(31)
UVO_5	3.67(1)	2.63(1)	2.05(1); 2.07(1)	2.27	(16)
UMo_2O_8	3.70(1)	2.60(1)	2.06(1); 2.06(1)	2.29	(33)
$U_2V_2O_{11}$	3.82(1)	2.67(1)	1.72(1); 1.77(1)	2.42	(20, 21)
$U_2P_2O_{10}$ (U^{VI}–U^{VI})	4.07(1)	2.77(1)	1.77(1); 1.77(1)	2.44	(35)
$U_2P_2O_{10}$ (U^{IV}–U^{IV})	4.09(1)	2.67(1)	2.17(1); 2.18(1)	2.38	
$U_2P_2O_{10}$ (U^{IV}–U^{VI})	4.03(1)	2.69(1)			
$USbO_5$	3.63(1)	2.60(2)	1.93(1); 2.03(1)	2.35	(32)
$H_2U_3O_{10}$	3.80(1)	2.60(1)	1.74(3); 1.78(3)	2.36	(36)

O(6) and O(7)); the O(6)–U(2)–O(7) angle shortened to 168(3)°. Refinements were also attempted in space groups $C2cm$ and $Cmc2_1$, and neither resulted in a satisfactory refinement.

The O(5) oxygen atoms of VO_4 tetrahedra of two parallel layers (Fig. 4) belong to the equatorial coordination of uranyl $U(2)O_2$ entities and are common to the two mirror-related $U(2)O_2$ moieties. Oxygen atoms of two water molecules $O(1)H_2$ also belong to the equatorial coordination of U(2). The values of the angles $O(5)$–U(2)–$H_2O(1)$ and $H_2O(1)$–U(2)–$H_2O(1)$ of 80° and 69°, respectively, are close to those in a regular pentagon (72°), but the fifth corner which should be in the mirror is missing from the Fourier difference syntheses. The coordinates of the $H_2O(3)$ oxygen atom in Table 2 are calculated so as to put this atom in the

ing U(2), O(6), and O(7) atoms. Actually, $U(2)O_2^{2+}$ uranyl ions half occupy two symmetrical positions related by the m-mirror parallel to the (001) plane. Furthermore the displacements of the U(2) atom in the (100) plane are very high (Table 3). In fact, the O(6) and O(7) atoms of one $U(2)O_2$ entity are very close to the $H_2O(3)^{iii}$ and $O(7)^{iii}$ atoms of the mirror-related $U(2)O_2$ group (0.60 and 0.90 Å, respectively) (Fig. 5), so the refined coordinates of O(6) and O(7) atoms are certainly erroneous. This could explained the too-short U=O bonds and the absence of an $H_2O(3)$ atom. Refinement with the O(6) site totally occupied (to take into account the presence of the $H_2O(3)$ molecule) and with the O(7) atom constrained in a 4c site (0, y, 1/4) (then the O(7) atom is common to the two mirror-related U(2)) led to the same reliability factors, to an increase of the O(6) and O(7) temperature factors (16(1) and 13(2) Å^2, respectively), and to higher U=O values (1.60(5) and 1.64(6) Å, respectively, for

FIG. 3. Relations between the triclinic cell (**a′**, **b′**, **c′**) of $U_2P_2O_{10}$ and the rectangular dimensions (a, b) of the layers in $U_3V_2O_{14} \cdot 5H_2O$.
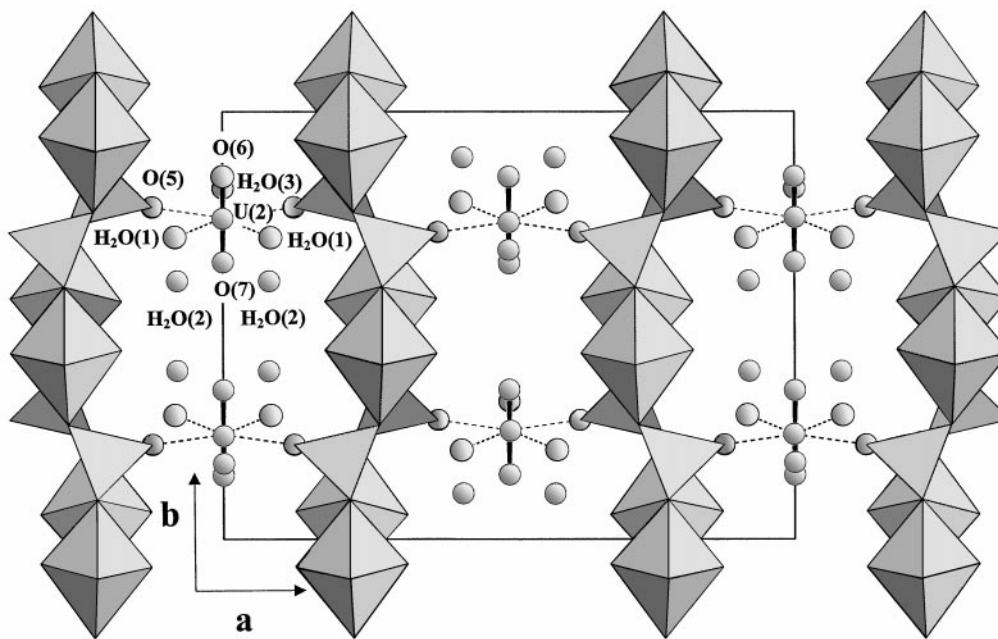
FIG. 4. The crystal structure of $U_3V_2O_{14} \cdot 5H_2O$ in [001] projection showing the connection of $(UVO_6)_\infty$ layers by uranyl ions.

O(5)–$H_2O(1)$–$H_2O(1)^{vi}$–$O(5)^{vi}$ plane at a distance of 2.43 Å from U(2).

Other water molecules, denoted $H_2O(2)$ (Fig. 2), are also situated in the interlayer space but are not coordinated to the U(2) atom. Its thermal displacement parameter is particularly high. However the oxygen–oxygen distances (Table 5) indicate hydrogen bonds.
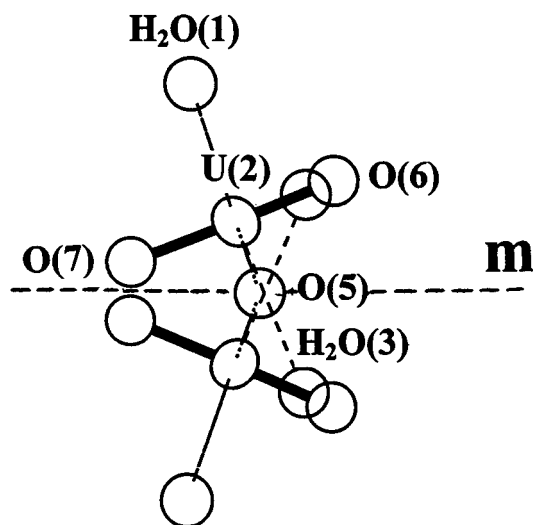
Finally, this compound may be considered a uranyl-vanadate of uranyl.

It is interesting to compare this uranyl vanadate with $(UO_2)_2(PO_4)_2 \cdot 4H_2O$, HUP, and its derived salts MUP. In the two types of compounds, the structure is composed of $[UO_2(XO_4)]_\infty$ layers (X = P, V) of XO_4 tetrahedra and uranyl ions separated by networks of cations and water molecules, but the association of uranyl and XO_4 ions differs. In HUP, uranyl ions are surrounded in the equatorial plane by four oxygen atoms from four different phosphate groups, resulting in a distorted octahedral coordination for uranium.
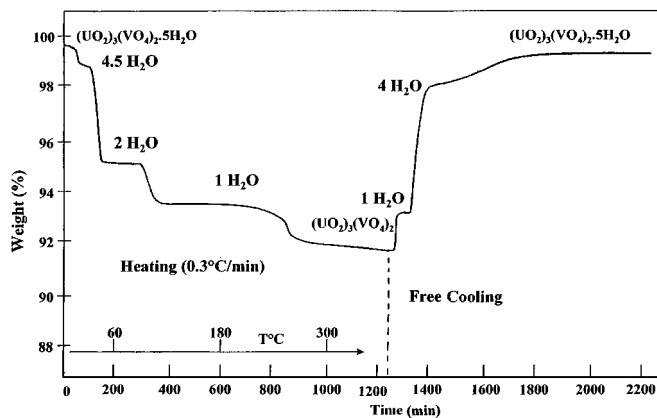

FIG. 5. The two *m*-mirror-related $U(2)O_7$ pentagonal bipyramids in $U_3V_2O_{14} \cdot 5H_2O$.

FIG. 6. Thermogravimetric analysis (TG) of $U_3V_2O_{14} \cdot 5H_2O$.
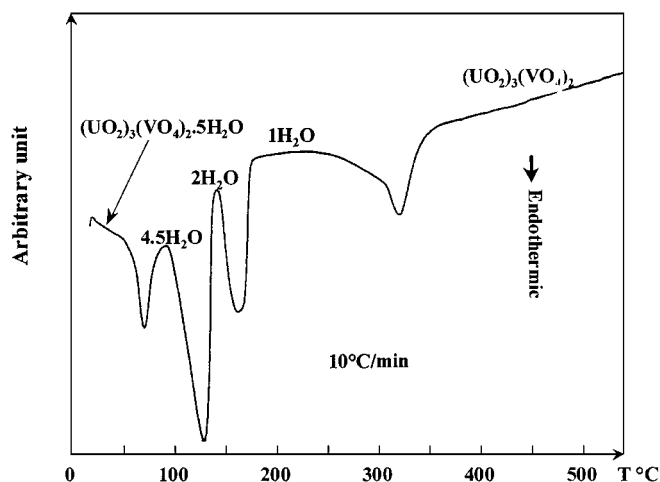
FIG. 7. Differential thermal analysis of $U_3V_2O_{14} \cdot 5H_2O$.

Thermal Stability

A thermogravimetric analysis has been performed on powder of $(UO_2)_3(VO_4)_2 \cdot 5H_2O$ previously dried under helium to prevent eventual adsorbed water molecules. The experimental curve is reported in Fig. 6. The $5H_2O$ per formula were confirmed, and several intermediates were in evidence, $(UO_2)_3(VO_4)_2 \cdot 4.5H_2O$, $(UO_2)_3(VO_4)_2 \cdot 2H_2O$, $(UO_2)_3(VO_4)_2 \cdot 1H_2O$.

The anhydrous compound $(UO_2)_3(VO_4)_2$ is unstable at room temperature in ambient air, and a fast rehydration process is evidenced, after cooling of the furnace, that leads

to $(UO_2)_3(VO_4)_2 \cdot 5H_2O$, via $(UO_2)_3(VO_4)_2 \cdot 1H_2O$ and $(UO_2)_3(VO_4)_2 \cdot 4H_2O$.

DSC measurements (Fig. 7) and high-temperature X ray powder diffraction (Fig. 8) are in agreement with the TG observations.

Direct synthesis by solid-state reaction from $UO_3 \cdot 1H_2O$ and V_2O_5 in stoichiometric amounts did not allow us to obtained the new $(UO_2)_3(VO_4)_2$ uranyl-vanadate. In agreement with previous works on the UO_3–V_2O_5 system, for temperatures lower than 500°C no reaction was observed; at 550°C, a mixture of UV_2O_8, γ-UO_3, and $U_2V_2O_{11}$ appeared; in the 700–750°C range, UV_2O_8 disappeared to give rise to a mixture of $U_2V_2O_{11}$ and U_3O_8.

CONCLUSION

Pentahydrated uranyl orthovanadate $(UO_2)_3(VO_4)_2 \cdot 5H_2O$ was synthesized and its crystal structure was determined. It may be considered a uranyl-vanadate of uranyl; in fact, its structure shows layers $(UVO_6)_\infty$ resulting from association of VO_4 tetrahedra and UO_7 pentagonal bipyramids sharing edges and corners. The layers are bridged together by other uranyl ions and water molecules. Similar layers are found in the mixed-valence uranium orthophosphate $U(UO_2)(PO_4)_2$.

Dehydration leads to the up to today unknown anhydrous orthovanadate $(UO_2)_3(VO_4)_2$, which cannot be directly synthesized by solid-state reaction. The crystal structure determination of this compound from high-temperature powder diffraction data is planned.

Interlayer uranyl ions are probably weakly bonded, and exchange reactions from this product to synthesize new layered compounds are in progress.
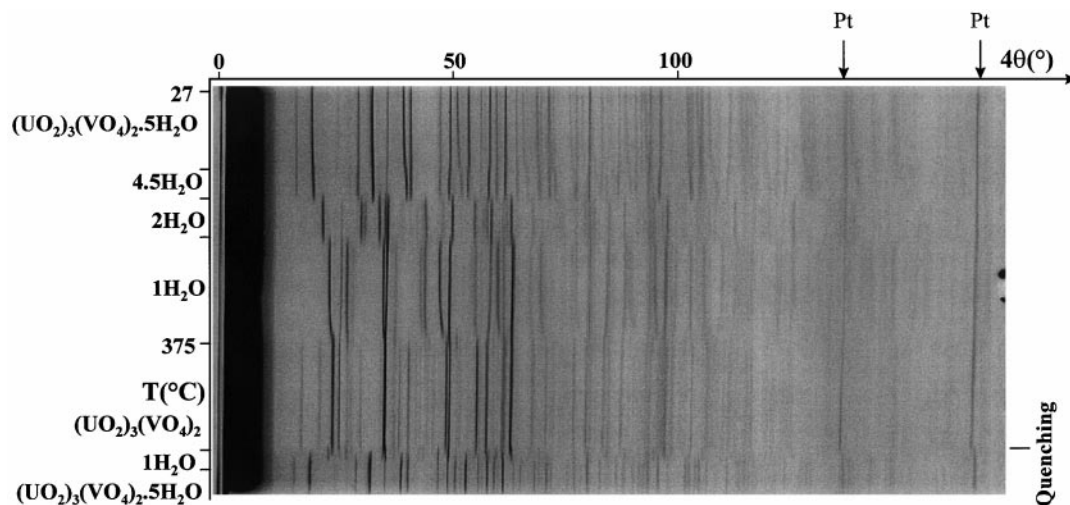

FIG. 8. High-temperature X-ray diffraction pattern of $U_3V_2O_{14} \cdot 5H_2O$.

REFERENCES

1. F. Weigel and G. Hoffman, *J. Less-Common Met.* **44,** 99 (1976).
2. B. Morosin, *Phys. Lett.* **65A,** 53 (1978).
3. D. E. Appleman and H. T. Evans, *J. Am. Miner.* **50,** 825 (1965).
4. F. Cesbron, Thesis, Paris 1970.
5. J. Borene and F. Cesbron, *Bull. Soc. Fr. Mineral. Cristallogr.* **93,** 426 (1970).
6. F. Abraham, C. Dion, and Mohamed Saadi, *J. Mater. Chem.* **3**(5), 459 (1993).
7. M. Pham-Thi, Ph. Colomban, and A. Novak, *J. Phys. Chem. Solids* **46**(5), 565 (1985).
8. M. Pham-Thi and Ph. Colomban, *Solid State Ionics* **17,** 295 (1985).
9. J. G. Kearley, *J. Mol. Struct.* **160,** 91 (1987).
10. A. N. Fitch and M. Cole, *Mater. Res. Bull.* **26,** 407 (1991).
11. P. B. Barton, *Am. Miner.* **43,** 799 (1958).
12. Von I. L. Botto and J. E. Baran, *Z. Anorg. Allg. Chem.* **426,** 321 (1976).
13. F. Abraham, C. Dion, N. Tancret, and M. Saadi, *Adv. Mater. Res.* **1–2,** 511 (1994).
14. J. C. Bobo, *Rev. Chim. Miner.* **4,** 4 (1964).
15. Shih-Hua Wang, L. M. Kovba, and V. I. Spitzyn, *Zh. Strukt. Kim.* **4**(5), 714 (1963).
16. P. G. Dickens, G. P. Stuttard, R. G. J. Ball, A. V. Powell, S. Hull, and S. Patat, *J. Mater. Chem.* **2**(2), 161 (1992).
17. A. M. Chippindale, S. J. Crennell, and P. G. Dickens, *J. Mater. Chem.* **3**(1), 33 (1993).
18. P. Pailleret, *C.R. Acad. Sci. Paris* **C265,** 1030 (1967).
19. P. Mahe-Pailleret, *Rev. Chim. Miner.* **7,** 807 (1970).
20. A. M. Chippindale, P. G. Dickens, G. J. Flynnand, and G. P. Stuttard, *J. Mater. Chem.* **5**(1), 141 (1995).
21. N. Tancret, S. Obbade, and F. Abraham, *Eur. J. Solid State Inorg. Chem.* **32,** 195 (1995).
22. L. M. Kovba, *Radiokhimiya* (*Engl. Transl.*) **13,** 940 (1971).
23. M. Gasperin and Chevalier, *Bull. Soc. Fr. Mineral. Cristallogr.* **93,** 18 (1970).
24. J. De Meuleaner and H. Tompa, *Acta Crystallogr.* **19,** 1014 (1965).
25. "International Tables for X-Ray Crystallography," Vol. IV. Kynoch Press, Birmingham, UK, 1974.
26. D. T. Cromer and D. Liberman, *J. Chem. Phys.* **53,** 1891 (1970).
27. C. T. Prewitt, SFLS-5, Report ORNL-TM 305. Oak Ridge National Laboratory, Oak Ridge, TN, 1966.
28. G. Smith and R. J. Snyder, *J. Appl. Crystallogr.* **12,** 60 (1979).
29. L. Pauling, "The Nature of the Chemical Bond," 3rd ed., p. 547. Cornell University Press, Ithaca, NY, 1960.
30. W. H. Bauer, *Am. Mineral.* **57,** 709 (1972).
31. B. O. Loopstra, *Acta Crystallogr.* **17,** 651 (1964).
32. P. G. Dickens and G. P. Stuttard, *J. Mater. Chem.* **2,** 691 (1992).
33. T. L Cremers, P. G. Eller, R. A. Penneman, and C. C. Herrick, *Acta Crystallogr.* **39,** 1163 (1983).
34. C. Askeljung and M. Sundberg, *J. Solid State Chem.* **144,** 152 (1999).
35. P. Benard, D. Loüer, N. Dacheux, V. Brandel, and M. Genet, *Chem. Mater.* **6,** 1049 (1994).
36. S. Siegel, A. Viste, H. R. Hoekstra, and B. Tani, *Acta Crystallogr.* **28,** 117 (1972).